QPF VERIFICATION AND BIMODAL PRECIPITATION PATTERNS OBSERVED AT WFO MORRISTOWN, TENNESSEE

David Matson

NOAA/National Weather Service Forecast Office
Morristown, Tennessee

Abstract

This paper investigates mean areal precipitation (MAP) climatology and tests the performance of quantitative precipitation forecasts (QPFs) issued by the National Weather Service Forecast Office at Morristown, TN (MRX) across the hydrologic service area (HSA). Results obtained are considered preliminary, as the time period under study was limited to 8.5 months (from mid-December 1998 through August 1999). Secondly, although operational QPF products are now issued from the Hydrometeorological Prediction Center (HPC) of the National Centers for Environmental Prediction (NCEP), this paper focuses on the short-term (1-6 hour) QPF problem where National Weather Service, Weather Forecast Offices (WFOs) can provide valuable insight.

QPFs demonstrated more skill (or lower error) when lighter rainfall events occurred. During the summer season, mean absolute error (MAE) of QPF was higher for nearly all prescribed ranges of MAP, citing the convective QPF as most problematic. MAP climatology, which identified the southeastern MRX HSA for more significant rainfall, was strongly influenced by synoptic-scale systems producing upslope flow events. Thus, the climatological MAP was divided into synoptic- and convective-scale (or bimodal) precipitation events. Results obtained for heavy rainfall cases (6-hour MAPs ≥ 0.50 in.) using this approach revealed different spatial precipitation patterns, each owing to a different dependence meteorologically. For diurnal convective systems, a temporal link was observed between frequency maxima and high levels of MAE along two interfaces: the Great Tennessee Valley and the adjacent Appalachian Mountains to the east, and, for synoptic systems, the largest frequency gradient and MAE occurred along the northern interface.

1. Introduction

Advances in hydrologic services provided by the National Weather Service (NWS) to the public into the twenty-first century will, in large measure, depend upon a better understanding of local precipitation patterns at NWS Weather Forecast Offices (WFOs). This is especially true at WFO Morristown (MRX), since the forecast office is a so-called "spin-up" facility under the Modernization and Restructuring (MAR) project, with little pre-MAR documented research on local precipitation in the Hydrologic Service Area (HSA). An integral part of additive local precipitation knowledge at MRX came from the Quantative Precipitation Forecasting (QPF) program once local software was developed.

Since the QPF program's inception into the NWS in 1995 under phase I of the MAR project, WFOs produced a QPF on a routine basis for river basins in their HSA. These were issued twice daily for hydrologic model input at the regional River Forecast Centers (RFCs). These QPFs included four 6-hour forecasts (and a 24-hour summed forecast from all 6-hour forecasts) for HSA river basin segments. RFC-generated Mean Areal Precipitation (MAP) data, generated once daily with temporal resolution paralleling QPF, provided calculated basin-average precipitation from observed data for each river basin segment. Thus, QPF and MAP data provided a means for QPF verification at the WFO level. However, an internal evaluation of the QPF program (1999) showed that WFO preparation and dissemination of QPF products consumed more man hours than at the centralized Hydrometeorological Prediction Center (HPC), and that selected WFOs showed no improvement against national QPF products issued at HPC. So, responsibility for the preparation of operational QPF transferred from the WFO to HPC in September 2000.

Despite advances in computer hardware and software systems in recent years, one of the most challenging assignments for meteorological forecasters is to accurately forecast precipitation. Part of this difficulty stems from the fact that mesoscale atmospheric influences occur in precipitation systems. One of the NWS vision goals by 2005 is for WFOs to implement a weather research and forecast model on the mesoscale. This will provide additional information to forecasters for predicting precipitation that could improve the short-term QPF problem.

This study documents precipitation knowledge gained at MRX as a result of implementing a locally-derived QPF verification program. Several statistical tools were used to provide insight into the spatial and temporal climatology of MAP and the accuracy of QPFs. MAP climatologies will be compared to the spatial precipitation patterns that emerged from thirty years of cooperative station data across the MRX HSA in Gaffin and Hotz (1999). A potentially more expressive synoptic- and convective-scale (bimodal) approach to precipitation climatology will be explored. However, results obtained in this study are considered preliminary, since the data set was limited to 8.5 months.

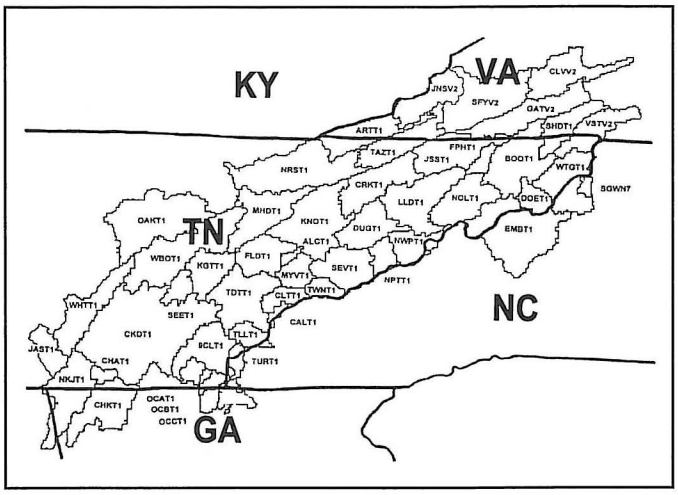

Fig. 1. The MRX HSA basins are shown; bold lines represent state boundaries.

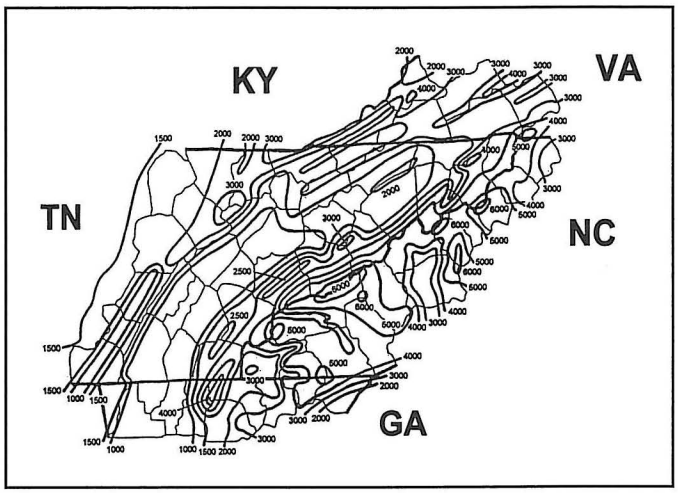

Fig. 2. Contoured elevations (in feet MSL) across the MRX HSA on a county map.

2. Data and Approach

MRX forecasters were responsible for issuing QPFs for the river basins (hereafter basins) of the MRX HSA. This includes all of eastern Tennessee, and sections of southwest Virginia, extreme western North Carolina, and northern Georgia (Fig. 1). QPFs were routinely generated twice daily using PC-based WinQPF software. WinQPF allowed forecasters to draw isohyets (contours of equal precipitation) across a pre-configured HSA grid at four 6-hour intervals and, from these, a 24-hour accumulation (i.e., five maps) was produced. When the forecaster completed a particular map, the software performed isohyetal analysis calculations on the grid. In this study, four 6-hour forecast intervals, beginning at 1200 UTC and ending at 1200 UTC the following day, and the 24-hour forecast sum ending at 1200 UTC, comprised the forecast data set.

MAP data sets were generated by hydrologic software at the RFC office in Slidell, LA which employed the Thiessen method (Linsley et al. 1986) to compute basin average precipitation from observed data. The MAP data provides the basis for a local precipitation climatology, whereas QPF data render the forecast.

In this study, all basin specific 6- and 24-hour RFC-produced MAP of 0.01 in.or more and their corresponding MRX-produced QPF comprised the verification data set. The time period of MAP and QPF data under study was from 1200 UTC 15 Dec 1998 through 1200 UTC 31 Aug 1999.

3. Topography

The topography across the MRX HSA varies significantly, ranging from mountainous peaks above 6500 ft mean sea level (MSL) in the southern Appalachian to elevations below 1000 ft MSL in some valleys (Fig. 2). Major topographical features in the MRX HSA include: 1) the Great Tennessee Valley (from northwest Georgia into southwest Virginia; 2) the Clinch and Powell mountains mainly in southwest Virginia; 3) the Blue Ridge mountains in northeast Tennessee and northwest North Carolina; 4) the Cumberland Plateau, west of the Great Tennessee Valley; and 5) the Sequatchie Valley. In Tennessee, the larger and more commonly known population centers of Chattanooga, Knoxville and the Tri-Cities region (the three cities of Bristol, Johnson City, and Kingsport) are all located in the Great Tennessee Valley.

4. Frequency Distribution of 6-hour and 24-hour MAP Basin Composites

A frequency distribution of 6-hour and 24-hour MAP amounts of 0.01-0.09 in., 0.10-0.24 in., 0.25-0.49 in., 0.50-0.99 in., 1.00-1.99 in., and ≥ 2.00 in. is featured in Fig. 3 (expressed in percentile). As MAP range increments increase (along the abscissa, from left to right), the number of 6-hour events decline markedly (from greater than 60% in the lightest range to less than 1% in the highest range). Logically, since four consecutive 6-hour MAPs comprise a 24-hour MAP, less change was observed with the 24-hour MAP, implying that rain events on average exceed six hours in duration. The composite sample sizes of 6- and 24-hour MAPs in this study, using the six discrete ranges in Fig. 3, are shown in Fig. 4.

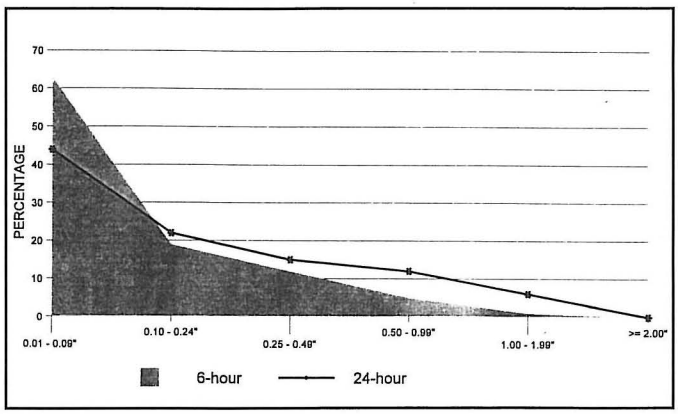

Fig. 3. Frequency distribution of 6-h and 24-h MAP (expressed as a percentage) displayed as a function of rainfall ranges (in inches) along the abscissa.

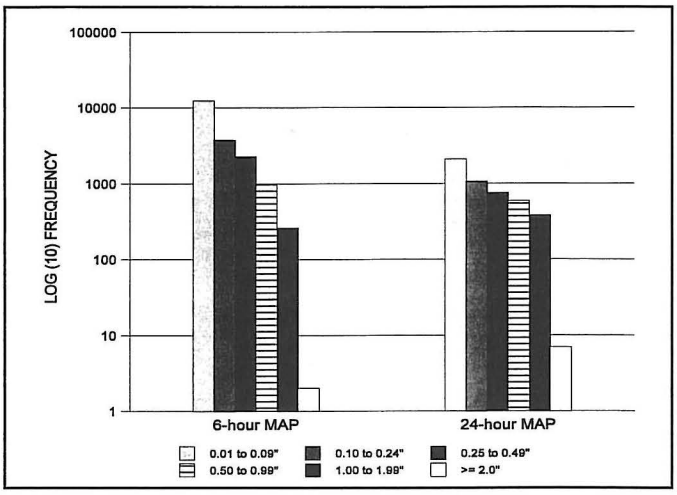

Fig. 4. Frequency of MRX HSA 6-h and 24-h MAP accumulations.

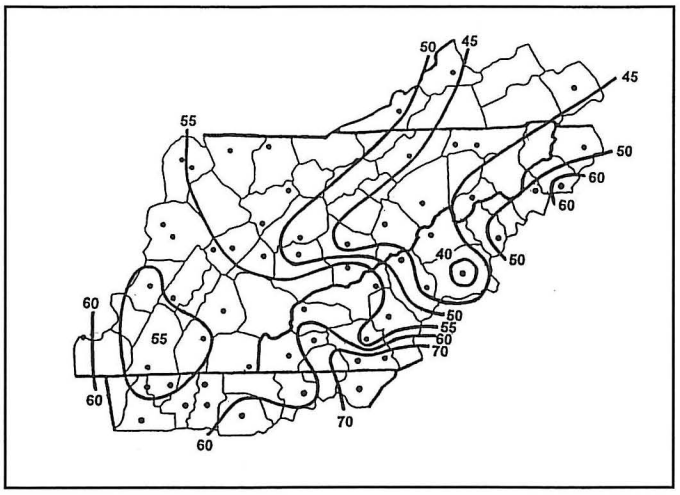

Fig. 6. Spatial distribution of annual rainfall (in inches) across the MRX HSA from Gaffin and Hotz (1999).

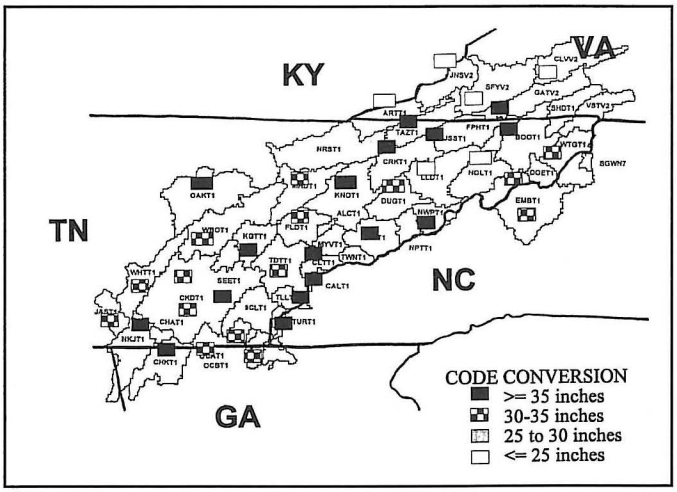

Fig. 5. Spatial distribution of 24-h MAP accumulations across MRX HSA basins.

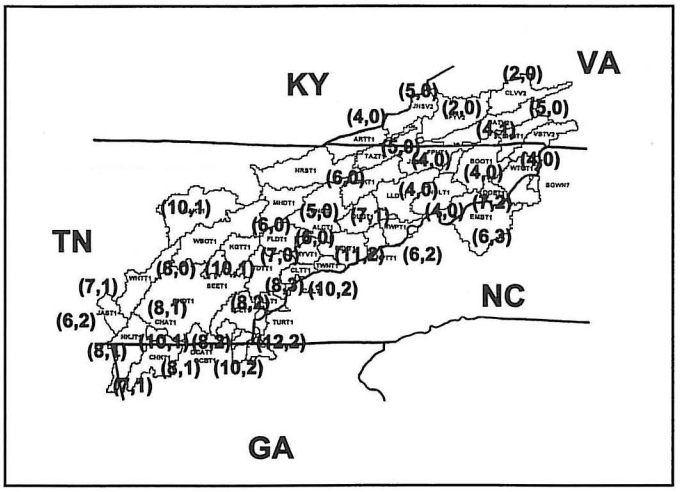

Fig. 7. Frequency distribution of 24-h MAP expressed as (x,y) at MRX HSA basins. X is frequency of rainfall events between 1.00 – 1.99 in.; y is frequency of events ≥ 2 in.

5. Composited MAP and QPF Verification

a. Spatial MAP

A spatial distribution of MRX 24-hour MAP accumulations at basins where data were available through the period under study was amassed, indicating significant regional precipitation variability (Fig. 5). A spatially coherent precipitation maximum was observed in the southeast MRX HSA, presumably due to higher elevations associated with the southern Appalachian chain, from extreme southeast Tennessee into southwest North Carolina (Fig. 2). One rationale for this regional precipitation maximum and the MRX HSA variability is that winter and transitional season precipitation systems tend to develop deep southerly flow, enhancing moisture transport and upslope flow to augment the precipitation process. A subset of this region, positioned at the north end, is the Smoky Mountains. This area hosts the highest mean elevation across the MRX HSA and, considering that the Blue Ridge Mountains in northeast Tennessee and northwest North Carolina receive less rainfall, appears to be a northern boundary for heavier mountainous precipitation. Elsewhere, the large-scale picture indicates that stabilizing downslope flow fosters a broad precipitation reduction.

It was previously documented that the MRX HSA topographical variation has a significant impact on annual precipitation distributions (Gaffin and Hotz 1999), shown graphically in Fig. 6. In fact, it is reassuring that the temporally limited MAP data set under study compares favorably in a general sense to the 30-year spatial distribution of precipitation from cooperative stations reported in Gaffin and Hotz (1999).

A frequency distribution of rainfall events from 24-hour MAP data ≥1.00 in. that occurred in the MRX HSA during the period under study (grouped into ranges of 1.00-1.99 in. and ≥ 2.00 in.) are presented in Fig. 7. According to Fig. 7, the spatial maximum occurred in the southeast MRX HSA. Farther north, the effects of localized upslope flow on precipitation systems across the Blue Ridge in northeast Tennessee and northwest North

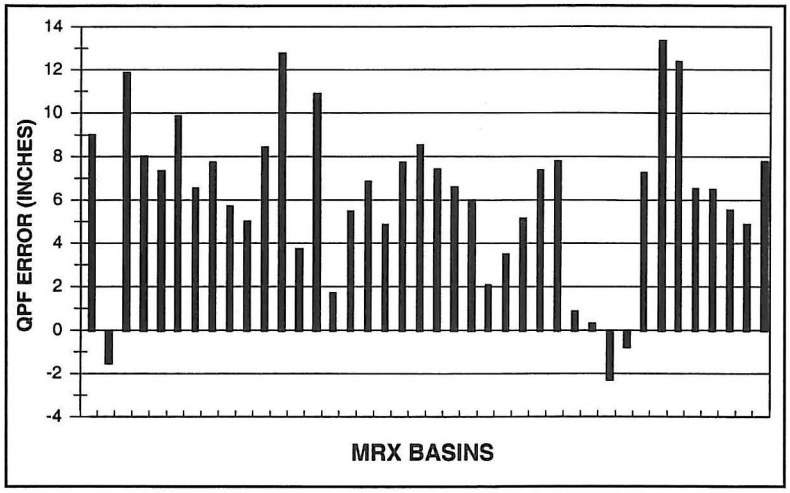

Fig. 8. Distribution of 24-h QPF errors (QPF – MAP) at MRX HSA basins.

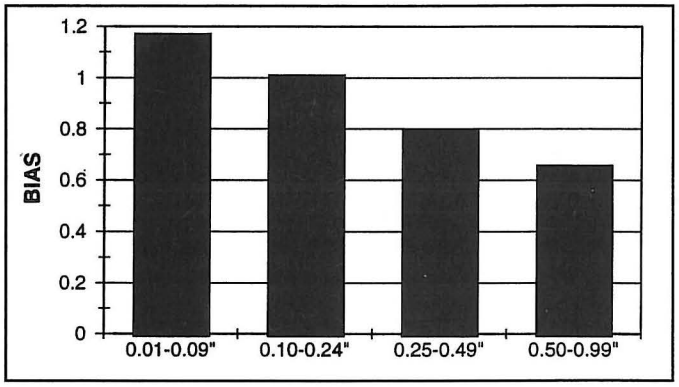

Fig. 9a. Mean 6-h QPF bias for four MAP ranges.

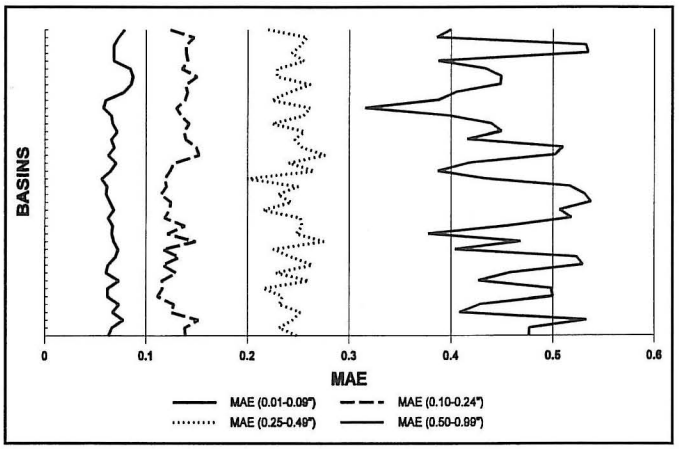

Fig. 9b. The 6-h QPF MAE for four MAP ranges.

Carolina aided in a few rainfall events ≥ 2.00 in. Whereas, to the west, large-scale downsloping across the central and northern Great Tennessee Valley provided for less frequent "heavy" rainfall events. This spatial distribution for heavy rainfall in the southeast MRX HSA is consistent with information obtained from the *Rainfall Frequency Atlas of the United States*, compiled by the Weather Bureau (1961). Thus, it appears the greatest threat for flooding rains is associated with orographic upslope flow, mainly in the southeast. However, results from the Gaffin and Hotz (1999) study do not identify this region as being most vulnerable to flash or prolonged flooding after reviewing 30 years of flash flood statistics in Storm Data. The combination of a low population density and a coarser spotter network in the southeast is believed to be the reason for this conflict.

b. Spatial QPF verification

Calculated 24-hour QPF error (QPF minus MAP) summed at most MRX HSA basins (where MAP and QPF data were complete for the period under study) indicate that MRX forecasters overpredict basin average rainfall amounts (Fig. 8), with a mean overprediction of nearly seven inches. The preponderance of QPF exceeding MAP amounts reported here is consistent with results reported in Mach and Hohman.

To determine the magnitude of QPF error, and measure QPF partiality, mean absolute error (MAE) and bias of QPF were calculated; as defined by eq. 1 and 2, respectively.

$$MAE = 1/N \ \Sigma \ | \ QPF - MAP \ | \qquad (1)$$

$$BIAS = 1/N \ (\Sigma \ NY + \Sigma \ YY \ ) / (\Sigma \ YY + \Sigma \ YN) \ ) \qquad (2)$$

where
YY=1 if QPF ≥ 0.01 in. and MAP ≥ 0.01 in.
NY=1 if QPF > MAP
YN=1 if MAP > QPF

Spatial and temporal averaging of 6-hour QPF bias, expressed as a function of four MAP ranges, was used to measure the ability of forecasters to predict rainfall in MRX HSA basins, displayed in Fig. 9a. Although there was some bias variability from basin to basin (not shown), their differences (for a given MAP range) were not considered significant. Wet biases (bias greater than unity) occurred when MAP amounts were < 0.10 in., and dry biases (bias less than unity) occurred when MAP amounts were ≥ 0.25 in. (Fig. 9a). In fact, QPF prediction of 6-hour precipitation amounts between 0.50 to 0.99 in. were very conservative (bias less than 0.7), and were even more conservative in predicting amounts ≥ 1.00 in. (not shown). Spatial MAE associated with 6-hour QPF, using the same four MAP ranges for bias in Fig. 9a, show larger MAEs (and MAE variances) when MAP thresholds increase, implying a major component of QPF error came from underpredicting heavier rainfall events or overpredicting the duration (Fig. 9b). Skill, inversely proportional to MAE, was considered relatively high when 6-hour precipitation amounts were less than 0.25 in., consistent with results in Mach and Hohman (1999). Also, this implies that forecasters were most proficient in determining which 6-hour time periods light precipitation would occur. As for heavier rain events, the tendency to underforecast can be attributed to their less frequent nature and from a tendency to distribute the rainfall amount (total) over multiple 6-hour time periods (Fig. 4).

c. Temporal MAP

A MRX HSA time series of 24-hour spatial-mean MAP is presented in Fig. 10. The time series exhibits a higher frequency of average MAP amounts exceeding 0.05 in. during the wintertime (when more widespread precipitation systems occur). Synoptic-scale disturbances are a central factor in developing winter and spring precipitation systems which typically bring the highest rainfall amounts to the MRX HSA (Gaffin and Hotz 1999). However, in this study, the 1999 springtime amplitudes were suppressed. During the summer season, three periods of widespread and heavy precipitation helped to alleviate a springtime deficit. Based on the amplitude of these summer precipitation events, the precipitation data may contain synoptic-scale contamination. This will be discussed before stratifying QPF verification into dominant modes of precipitation in Section 6a.

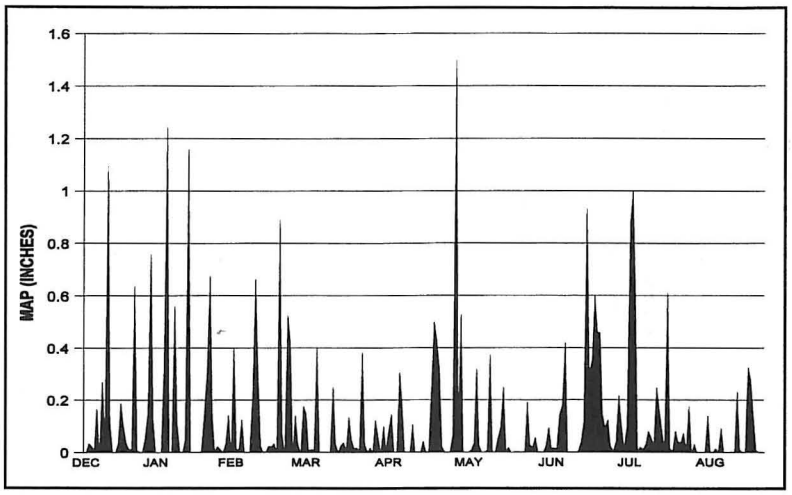

Fig. 10. Time series of 24-h MAP amounts (in.) over period studied.

d. Temporal QPF verification

Subsets of the 24-hour MAP data from Fig. 10 (for a portion of the winter and summer), overlaid with QPF error, are shown in Fig. 11a and b, respectively. For the winter events (Fig. 11a), QPF error demonstrates that MRX forecasters underforecasted a majority of "heavier" precipitation events, and that the QPF error gap generally increased when MAP amounts were greater. When "lighter" MAP amounts occurred (i.e., over-running precipitation systems), MRX forecasters tended to overforecast. The same prediction patterns during the wintertime emerged for summer events (Fig. 11b).

A frequency distribution of 6- and 24-hour spatial- and monthly-mean MAP amounts and MAE are exhibited in Fig. 12a and b, respectively. One of the findings was that light precipitation (0.01-0.09 in.) frequencies increased during the warm-season due to air mass showers and thunderstorms. Secondly, summertime-mean MAE was higher for all MAP ranges, especially when MAP exceeded 1.00 in. A rationale for these limitations stems from the fact that the most problematic QPF is the convective QPF (Doswell and Maddox 1986), because knowledge-based decisions regarding convective-scale precipitation processes are limited, and that most atmospheric models are not likely to perform consistently well during convective episodes.

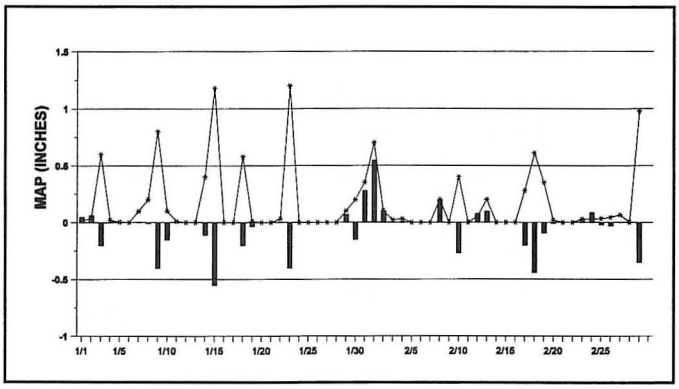

Fig. 11a. Time series of January and February 1999 MAP amounts (solid line) and QPF errors (bars).

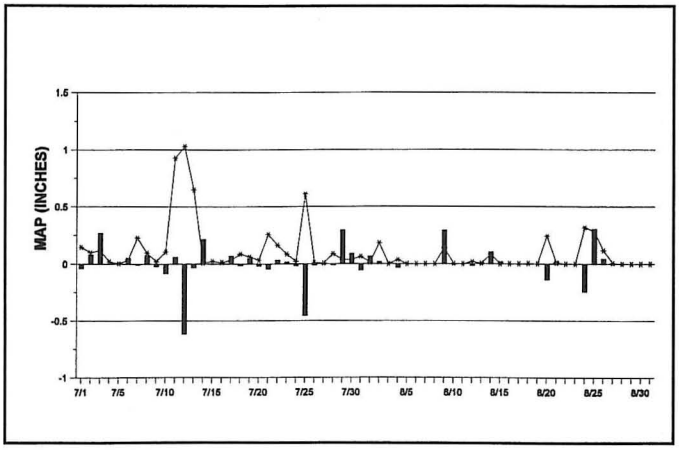

Fig. 11b. Time series of July and August 1999 MAP amounts (solid line) and QPF errors (bars).

6. Convective and Synoptic-Scale QPF Verification

a. Method of classification

Synoptic-scale forcing was considered the dominant mechanism for winter and springtime precipitation regimes. Precipitation for the summer season was considered convectively dominant, although a few periods of prolonged precipitation (exceeding the time-scale of convective storms) shown in Fig. 10 may have been influenced by cold fronts with strong tropospheric winds (i.e., synoptic-scale systems). In order to determine if this was so, MRX HSA basin-average 24-hour MAP values were operated on using a time-averaged temporal variance function (hereafter referred to as VSTAT, defined in eq. 3). Considering that basin rain gage resolution does not typically resolve the characteristic length-scale of convective storms and, by observing the characteristic 24-hour precipitation "spike" in basin-average MAP data during the winter and spring periods (Fig. 10), VSTAT measures the amplitude of the synoptic scales by differencing the

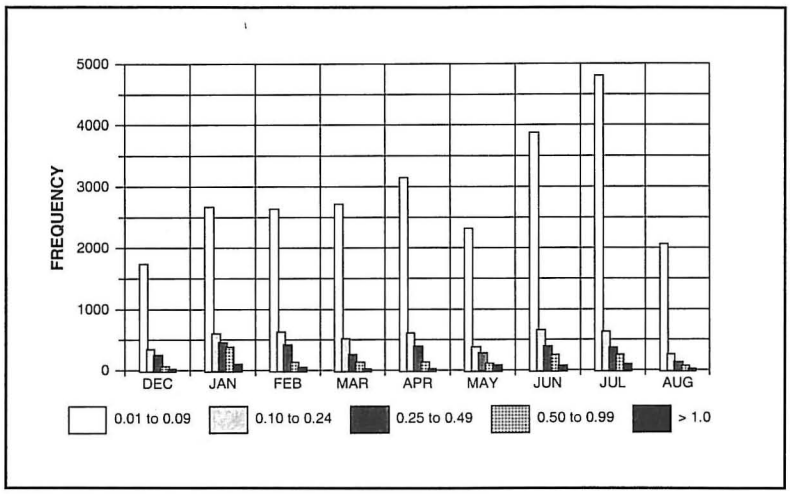

Fig. 12a. 6-h and 24-h MAP frequencies in five ranges over the months covered in study.

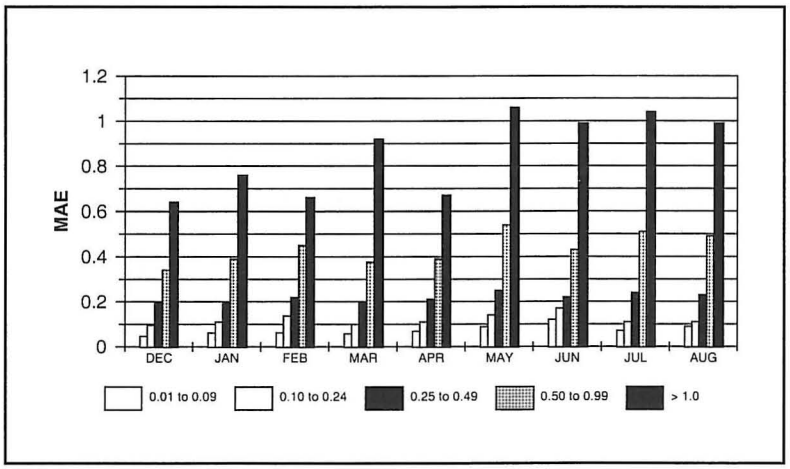

Fig. 12b. 6-h and 24-h MAP MAE frequencies in five ranges over the months covered in study.

24-hour HSA-average MAP amount from a 3-day mean HSA-average MAP amount ($x(t_i)$ and $x(t_j)$, respectively). Thus, higher (lower) values of VSTAT increase (decrease) the level of synoptic-scale influence in precipitation systems. Empirically setting VSTAT ≥ 0.01 identified a significant level of synoptic-scale contamination in summertime precipitation systems.

Calculated VSTAT, the VSTAT threshold of 0.01, and basin-average MAP amounts are displayed in Fig.13. It is observed that VSTAT anomalies occur more frequently in the winter-time, as expected. From VSTAT, three summertime precipitation episodes (as indicated by arrows in Fig. 13) displayed a significant amount of synoptic-scale contamination. As a result, MAP and QPF data for these events were transferred into the synoptic-scale precipitation mode.

$$VSTAT(t_i) = 1/N \Sigma \{[x(t_i) - x(t_j)]^2\}^{1/2} \quad (3)$$

where

t_i = date of 24-hour / 1200 UTC MAP

$x(t_i)$ = HSA-average MAP at t_i

$x(t_j)$ = 3-day (t_{i-1}, t_i and t_{i+1}) mean HSA-average MAP

N = total number of basins

b. Regional grouping of data

Data in this study henceforth will be presented regionally across the MRX HSA by grouping basins of similar topography together. Basin resolution was a factor in determining the regions, because the number of basins between regions should be balanced. As a result, eight regions were selected: (1) the Cumberland Plateau (CP); (2) the Southern Tennessee Valley (SV); (3) the Southern Appalachian Mountains (AM); (4) the Smoky Mountains (SM); (5) the Central Tennessee Valley (CV); (6) the Northern Tennessee Valley in Tennessee (NV); (7) the Northeast Mountains, principally in northeast Tennessee (NM); and (8) the Northern Tennessee Valley in Virginia (NA). These regions are displayed on the MRX HSA basin map (Fig. 14).

c. Regional statistical analysis

A broader classification scheme for MAP ranges was used on synoptic- and convective-scale 6-hour MAP amounts to verify QPFs. These range divisions for light, moderate, and heavy precipitation were selected as: (1) 0.01-0.24 in.; (2) 0.25-0.50 in.; and (3) > 0.50 in.; respectively.

Regional synoptic- and convective-scale, or bimodal, MAP frequencies are shown in Fig. 15a. For light precipitation frequency there was an analogous bimodal trend, featuring higher frequencies in mountainous regions (AM, SM and NM) with a peak in the NM region. Bimodal heavy rain events exhibited a frequency maximum in the SM region with a positive (negative) gradient south (north). Since the SM region hosts the highest mean and peak elevations in the MRX HSA, this underscores the importance of orographic feedback in precipitation systems, whether synoptically or convectively driven. However, there is a different dependence meteorologically to each mode. Synoptic systems are stronger dynamical systems, typically associated with moist southerly upslope flow while, for convective systems, the thermal structure of the troposphere is more important (i.e., lapse rates).

Regional bimodal 6-hour MAEs are shown in Fig. 15b. Light convective MAE indicated homo-geneous QPF skill across the MRX HSA whereas, for synoptic precipitation, slightly lower (higher) skill occurred in the south (north). Synoptic-scale heavy rainfall MAE maximas occurred in the SV and CV regions, indicating that downsloping effects in the precipitation process were forecast too conservatively. Convective precipitation systems that produced heavy rainfall yielded significantly higher MAE, with a southeast MRX HSA (SV, AM, SM, and CV) mean MAE near 0.7. Higher convective MAEs observed across the precipitation classification spectrum in nearly all regions was largely attributable to increased spatial variability with convective precipitation.

Bimodal QPF bias (Fig. 16), for light precipitation, shows slight convective wet biases in the SM and NV regions and only in the NV region for the synoptic-scales.

In contrast, moderate to heavy bimodal precipitation biases were well below unity. For heavy rainfall, the convective bias was, on average, close to a pure underprediction (bias=0.5) and, for synoptic-scale systems, more frequent wet biases occurred in the central and southern MRX HSA.

d. Basin statistical analysis for heavy rainfall

A more detailed (or higher resolution) statistical analysis was used for the more significant heavy rainfall cases to further probe the bimodal MAP frequency and MAE trends noted in section 6c. In Figs. 17-19, regional basins and basin data will be presented in a contiguous fashion, identified along the abscissa. Bimodal MAP frequencies and MAEs for 6-hour data were run through a smoothing operator to reduce basin-to-basin variability, calculated as a moving average between the central basin and its immediate neighbors (neighbor for end points).

Smoothed convective heavy rainfall MAP frequencies and MAEs (Figs. 17a and b, respectively) reveal that significant amplifications were in phase. Near the amplified states, there were two interfaces where rapid changes in heavy rainfall frequency occurred, one between the SV and AM regions (the SV/AM interface), and the other between the SM and CV regions (the SM/CV interface). Understanding the behavior at these interfaces is important because this was where higher MAEs occurred, particularly at the SM/CV interface maximum. Since the majority of convective storms across the MRX HSA were diurnal during the summer season under study, 6-hour MAP frequencies and MAE for convective storms producing heavy rain (terminating at 1800 UTC and 0000 UTC) were examined (Fig. 18).

An examination of 6-hour MAP frequencies for heavy convective rainfall ending at 1800 UTC (Fig. 18a) indicated that steady growth took place in the southern and central SM region (where the frequency peak occurred). The frequencies fall off rapidly in the northern SM region, and into the adjacent CV region. Successive 6-hour MAP frequencies ending at 0000 UTC expose a decay in the SM region maximum, and develop two coherent maximas in the SV and CV regions (Fig. 18b). The 1800 UTC maximum and the 0000 UTC convective frequency "split" in the SM region indicate that higher elevations of the Smoky Mountains more readily break overnight capping inversions and become convectively unstable in response to intense heating of the sun-facing slopes (and the ensuing mountain-valley circulation) by the late morning and early afternoon hours. Thunderstorms that form in weak vertical wind shear and moderate to high instability (CAPE ≥ 1500 J kg^{-1}, lifted indices ≤ -3) may produce heavy rainfall over a short period of time, bringing much colder and denser air to ground level (i.e., "cold pools"). This study suggests that dense fluid creat-

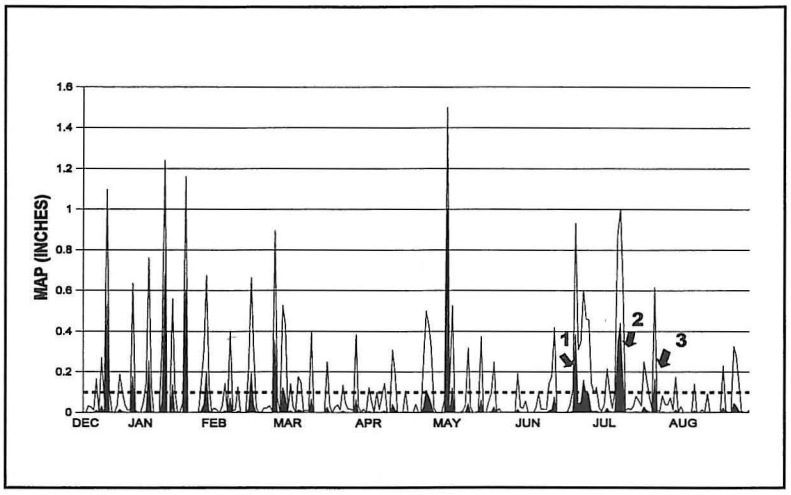

Fig. 13. Time series of 24-h mean MAP amounts (in.), VSTATs (area filled) and VSTAT = 0.1 (dashed horizontal line).

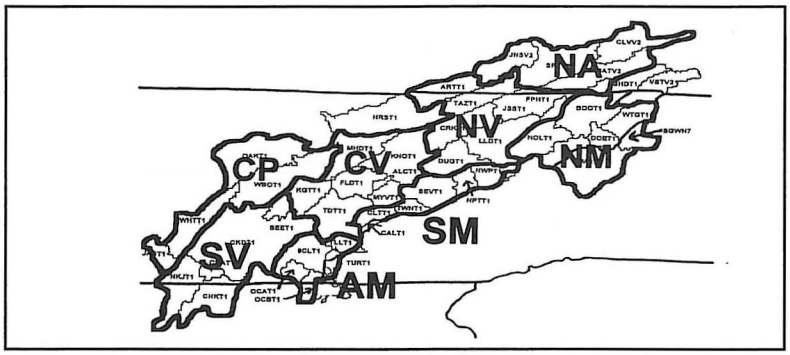

Fig. 14. Eight geographic regions featuring similar topography labeled and outlined across the MRX HSA basins (Fig. 1)

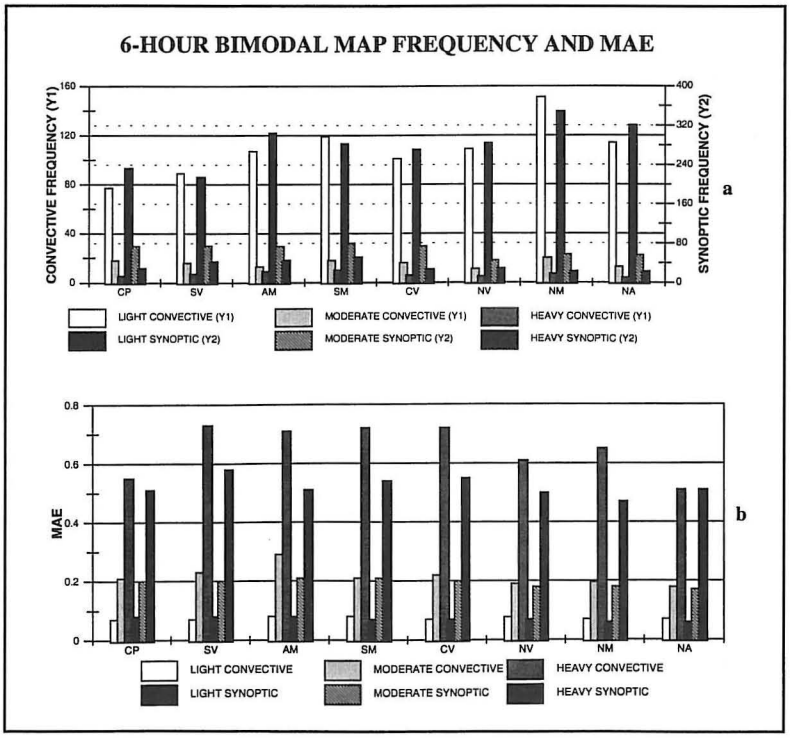

Fig. 15. 6-h bimodal MAP frequencies in (a) and MAE in (b) for the eight geographic regions in Fig. 14. Light, moderate and heavy precipitation were defined in ranges of 0.01-0.24 in., 0.25-0.50 in. and > 0.50 in. respectively.

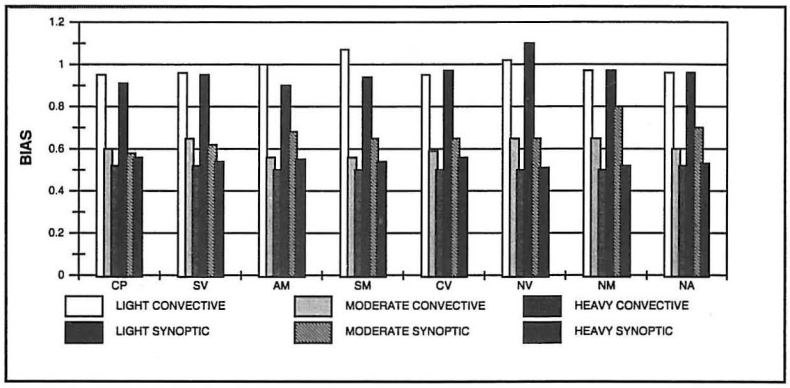

Fig. 16. As in Fig. 15, except depicting the 6-h bimodal bias for the eight geographic regions in Fig. 14.

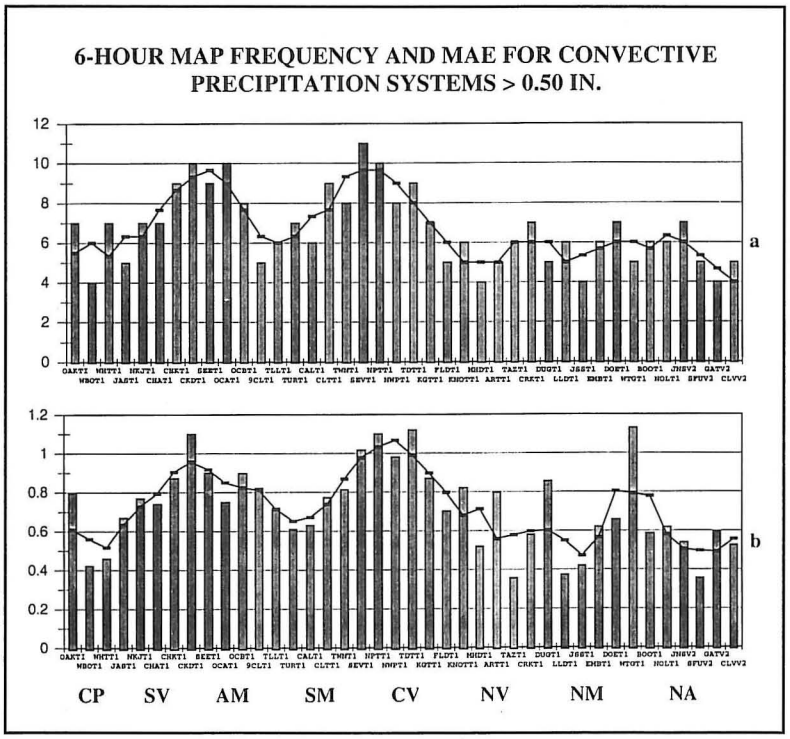

Fig. 17. Frequencies of the 6-h MAP amounts > 0.50 in. in (a) and MAE in (b) for convective precipitation systems in each of the MRX HSA basins aligned in their eight geographical regions.

ed by "cold pools" and the lighter fluid surrounding it generated a significant hydrostatic pressure gradient that drove a density current from the SM region into the central Tennessee Valley, accelerated by the gravitation force down western slopes along the SM/CV interface. In many cases, this triggered or enhanced heavy convective rainfall into central sections of the Tennessee Valley (near the SM/CV interface) before veering down-valley into the southern Tennessee Valley (creating the SV/AM interface).

When there was significant diurnal lag time between thunderstorms producing heavy rainfall in the Smoky Mountains (and the formation of a density current) and thunderstorm initiation in the Tennessee Valley, temperature differences normal to the density current inevitably mixed out and the pressure gradient decayed. However, residual quasi-stationary boundaries were left over, and thunderstorms tended to form first along these when surface temperatures reached their diurnal maximum. Such outflow boundaries can play a vital role in the initiation of subsequent convection, which may evolve into a quasi-stationary mesoscale convective system (MCS) as described in Chappell (1986).

Regional basins more susceptible to 6-hour heavy convective rainfall (SM basins from 1200 UTC to 1800 UTC, and SV and CV basins from 1800 UTC to 0000 UTC) were also a significant source of MAE (MAE comparison between Fig. 15b and Figs. 18a, b). This emphasizes the need to recognize and closely monitor mesoscale boundaries/currents and environmental changes conducive to heavy convective rainfall, especially in the SM, CV and SV regions where there appears to be a temporal link. Although there was a near equal distribution of 6-hour heavy precipitation events in the SV and CV regions by 0000 UTC, MRX forecasters were more confident that heavier rainfall would occur in the SV region since it typically hosts the most unstable late afternoon and evening summertime environment across the MRX HSA.

Heavy rainfall frequencies associated with synoptic-scale precipitation systems were less variable from basin to basin, depicting a more uniform distribution (Fig. 19a). However, a rapid reduction in frequencies occurred across the SM/CV interface where the central SM region (highest peaks in elevation across the MRX HSA) acted as an effective northern boundary for more frequent heavy rain events. The rapid frequency decline into the CV region was attributed to downsloping. On average, for synoptic-scale systems, the southern MRX HSA received nearly twenty more heavy rain episodes. Heavy rainfall MAEs associated with synoptic-scale systems were greatest along the SM/CV interface (Fig. 19b).

MAP climatology and frequency distributions of 24-hour heavy rainfall in the MRX HSA (Fig. 5 and 7, respectively) were highly influenced by more frequent synoptic-scale precipitation systems in this study. Since it was reported that the majority of flash flood events across the MRX HSA are convectively driven (Gaffin and Hotz 1999), and considering convective frequencies for heavy rainfall in Figs. 17a and 18a-b, it appears that the flash flood threat in the southeastern MRX HSA (or largely the AM region) may not be as high as the adjacent regions north and west.

7. Summary and Conclusions

Spatial QPF verification indicated that 24-hour QPFs were overpredicted in nearly all MRX HSA basins. QPF biases were mostly > 1.0 when measurable MAP amounts were < 0.25 in., and were < 1.0 when MAP amounts were ≥ 0.25 in. Temporal QPF verification indicated that summertime-mean MAE was higher for all ranges of MAP, most notably when MAP amounts were > 1.00 in.

The MAP climatology of MRX HSA basins for the limited time period under study revealed a strong orographic signal during synoptic events, featuring heavier rainfall in the southeast associated with upslope flow, and generally lighter amounts elsewhere from downsloping. This finding is in general agreement with the annual precipitation climatology reported in Gaffin and Hotz (1999).

MAP climatology was adjusted for synoptic (winter and transitional seasons) and convective (summertime) modes of light, moderate, and heavy precipitation, grouped into eight regions where the topographic character is similar. An adjustment was made for a few summertime events that contained a high level of synoptic-scale contamination. Synoptic- and convective-scale (or bimodal) frequencies for light rain (0.01-0.25 in.) were highest in the Northeast Mountain (NM) region and frequencies for heavy rain (> 0.50 in.) peaked in the Smoky Mountain (SM) region (highest elevations in the MRX HSA). Convective precipitation systems that produced heavy rainfall had considerably higher MAEs and lower biases relative to the synoptic precipitation systems across MRX HSA. A closer inspection of the more significant heavy rain events revealed additional bimodal differences. Spatial frequencies of synoptic-scale systems were more uniform across the MRX HSA, other than for a rapid reduction along the SM/CV interface where the MAE maximum occurred (suggesting that the effects from downsloping were forecast to conservatively). Whereas, for convective systems, frequency maximas and high MAEs occurred along the SV/AM and SM/CV interfaces.

It is proposed that diurnal heavy rainfall events for convective systems tended to form first over the SM region. That in turn generated a hydrostatic pressure gradient force sufficient enough to drive a density current into the Tennessee Valley, which accelerated by gravity down western slopes into the CV region. If thunderstorm cells developed along the density current (or residual quasi-stationary boundaries) in a moist and unstable atmosphere with little wind shear, they were likely to produce heavy rainfall in the CV and SV regions. The high levels of MAE along the SV/AM and SM/CV interfaces stress the need for forecasters to recognize and closely monitor mesoscale boundaries/currents and environmental changes conducive to heavy convective rainfall in these areas.

MAP climatology and heavy rainfall frequencies across the MRX HSA suggest that the southeast (or largely the AM region) is more prone to flooding. However, larger sample sizes of synoptic-scale precipitation were found to bias the climatological MAP. Although MAP climatology (whether annual, seasonal, or monthly) may be considered helpful to formulate a QPF, results obtained in this study suggest that a synoptic- and convective-scale approach may provide for more definitive information. Forecasters need to be aware of areas which are more susceptible to heavy rainfall (and potential flooding) as a function of the mode of forcing. For example, if a forecaster believes that there is a threat for convectively forced heavy rainfall in the MRX HSA,

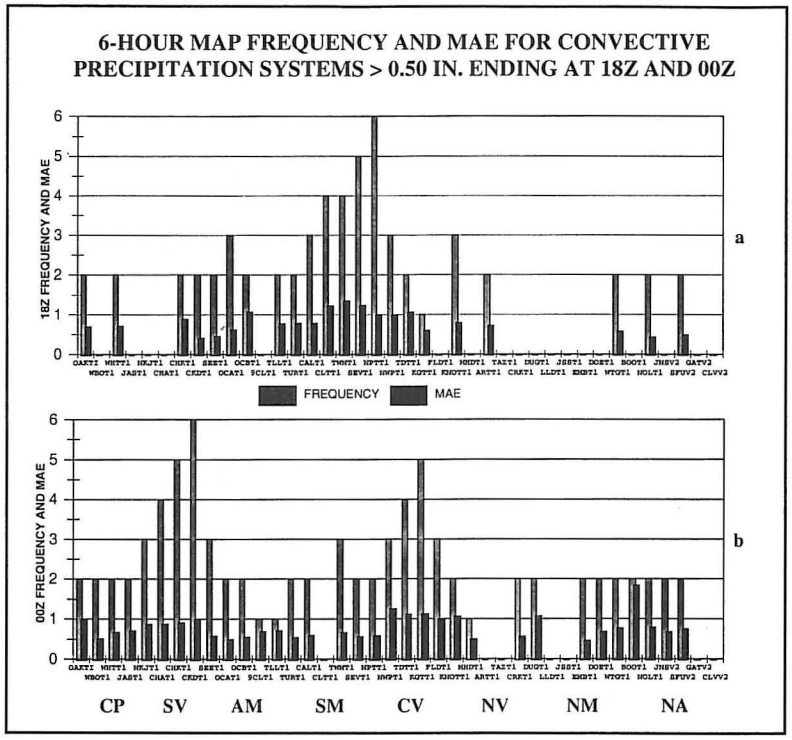

Fig. 18. Frequencies of the 6-h MAP amounts > 0.50 in. and MAE for convective precipitation systems in each of the MRX HSA basins aligned in their eight geographical regions for 1200-1800 UTC in (a) and 1800-0000 UTC in (b).

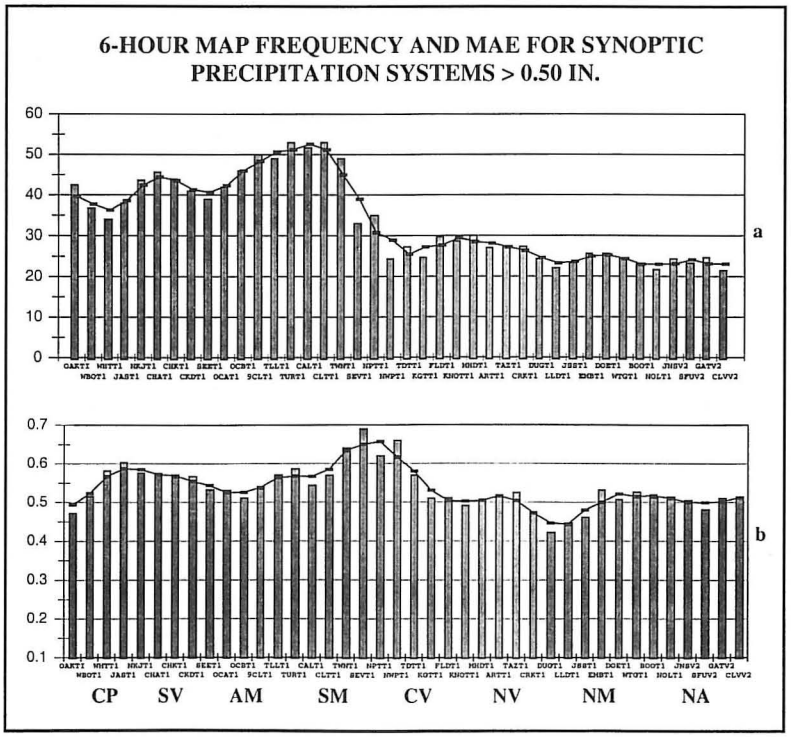

Fig. 19. As in Fig. 17, except for synoptic precipitation systems.

the summertime flash flood focus could shift into the CV, SV and SM regions of the MRX HSA. Conversely, river or long-term (in excess of six hours) flooding is more likely in the southeastern MRX HSA during the winter and early spring when low evapo-transpiration rates, snow melt, and the linkage between upslope flow and heavy rainfall occurs with synoptic-scale systems.

Acknowledgments

The author would like to thank Brian Boyd, Service Hydrologist, and Stephen Parker, Science and Operations Officer, at WFO Morristown, Tennessee, for their suggestions and later reviews of this document. Also, the author would like to thank the reviewers of NWD, David E. Stooksbury and Mike Gillen, for their refinements to this article.

Author

David Matson received the B.S. and M.S. degrees in Meteorology from Texas A&M University late in 1991 and 1993, respectively. He joined the NWS in Oct 1993 as a meteorological intern at the NWS Office in Augusta, GA and transferred to the NWS Little Rock Office in Dec 1995. He was promoted to journeyman forecaster at the NWS Forecast Office in Morristown, TN in Sept 1998. His meteorological interests vary from planetary-scale phenomenon such as blocking flows and teleconnective patterns down to convective-scale phenomenon such as thunderstorm complexes that produce flash flooding and severe weather. His last published article appeared in the *National Weather Digest* in June 1998. That article presented the methodology used to optimize the WSR-88D Doppler Radar system adaptable parameter set in the MESO/TVS algorithm from more skillful TVS detections under Build 9 at the NWS Little Rock Office.

References

Chappell, C.F., 1986: *Quasi-Stationary Convective Events. Mesoscale Meteorology and Forecasting*, P.S. Ray, ed., Amer. Meteor. Soc., 289-310.

Doswell, C. A., III, and R. A. Maddox, 1986: The Practical Realities of QPF. *NOAA Technical Memorandum*, NWS SR-117, 1986 NWS Southern Region QPF Workshop, 8-12 pp.

Gaffin, D. M., and D. G. Hotz, 2000: A Precipitation and Flash Flood Climatology of the WFO Morristown, Tennessee Hydrological Service Area. *NOAA Technical Memorandum*, NWS SR-204, 1-24 pp.

Lindsey, R. K., M. A. Kohler, and J. L. H. Paulhus, 1986: *Hydrology for Engineers, Third Edition*. McGraw-Hill, Inc., New York, 70-74 pp.

Mach, M. A., and W. Hohman, 1999: A Preliminary Evaluation of a Verification Scheme to Compare Mean Areal Precipitation to Local Quantative Precipitation Forecasts During Widespread Rainfall Events. *NOAA Technical Memorandum*, NWS SR-200, 12 pp.